Materials Advances

ROYAL SOCIETY OF CHEMISTRY

PAPER

View Article Online
View Journal | View Issue



Cite this: *Mater. Adv.*, 2024, 5, 8575

# The effect of low temperature on poly(3-methyl-*N*-vinylcaprolactam)-*b*-poly(*N*-vinylpyrrolidone) diblock copolymer nanovesicles assembled from all-aqueous media†

Veronika Kozlovskaya, ‡[a] Yiming Yang,‡[a] Shuo Qian [b] and Eugenia Kharlampieva *[ac]

Nanosized polymeric vesicles (polymersomes) self-assembled from double hydrophilic copolymers of poly(3-methyl-*N*-vinylcaprolactam)$_n$-*b*-poly(*N*-vinylpyrrolidone)$_m$ (PMVC$_n$-*b*-PVPON$_m$) using all aqueous media are a promising platform for biomedical applications, because of their superior stability over liposomes *in vivo* and high loading capacity. Herein, we explored the temperature-sensitive behavior of PMVC$_{58}$-*b*-PVPON$_{65}$ vesicles using transmission electron microscopy (TEM), dynamic light scattering (DLS), atomic force microscopy (AFM), and small-angle neutron scattering (SANS) in response to lowering the solution temperature from 37 to 25, 20, 14 and 4 °C. The copolymer vesicles with an average size of 350 nm at 37 °C were assembled from the diblock copolymer dissolved in aqueous solution at 4 °C. We show that while the polymersome's size gradually decreases upon the temperature decrease from 37 to 4 °C, the average shell thickness increases from 17 nm to 25 nm, respectively. SANS study revealed that the PMVC$_{58}$-*b*-PVPON$_{65}$ vesicle undergoes a gradual structure evolution from a dense-shell vesicle at 37–25 °C to a highly-hydrated shell vesicle at 20–14 °C to molecular chain aggregates at 4 °C. From SANS contrast matching study, this vesicle behavior is found to be driven by the gradual rehydration of PMVC block at 37–14 °C. The shell hydration at 20–14 °C also correlated with the 4.4-fold decrease in the relative fluorescence intensity from vesicle-encapsulated fluorescent dye, indicating ~80% of the dye release within 12 hours after the vesicle exposure to 14 °C. No significant (<5%) dye release was observed for the vesicle solutions at 37–20 °C, indicating excellent cargo retention inside the vesicles. Our study provides new fundamental insights on temperature-sensitive polymer vesicles and demonstrates that the copolymer assembly into polymersomes can be achieved by decreasing a copolymer aqueous solution temperature below 14 °C followed by solution exposure to ≥20 °C. This type of all-aqueous assembly, instead of nanoprecipitation from organic solvents or solvent exchange, can be highly desirable for encapsulating a wide range of biological molecules, including proteins, peptides, and nucleic acids, into stable polymer vesicles without a need for organic solvents for dissolution of the copolymers that are amphiphilic at physiologically relevant temperatures of 20–37 °C.

Received 18th August 2024,
Accepted 1st October 2024

DOI: 10.1039/d4ma00831f

rsc.li/materials-advances

## 1. Introduction

Unilamellar polymer vesicles, also known as polymersomes, are capsule-like structures assembled from amphiphilic block copolymers consisting of a soft bilayer membrane and a hollow interior. They have attracted much attention as promising tools for encapsulation, storage, and target delivery of therapeutic and other functional molecules.[1–4] In contrast to liposomal vesicles assembled from phospholipids that may suffer from low physical integrity causing cargo leakage,[5] easy fusion,[6] low oxidative stability,[7] and limited functionalities,[8] polymer vesicles assembled from block copolymers demonstrate various

[a] *Chemistry Department, The University of Alabama at Birmingham, Birmingham, Alabama, 35294, USA. E-mail: ekharlam@uab.edu*
[b] *Neutron Scattering Division, Neutron Sciences Directorate, Oak Ridge National Laboratory, Oak Ridge, Tennessee 37831, USA*
[c] *Center for Nanoscale Materials and Biointegration, The University of Alabama at Birmingham, Birmingham, Alabama, USA 35294*

† Electronic supplementary information (ESI) available: $^1$H NMR spectra of 3-methyl-*N*-vinylcaprolactam monomer, methyl 2-((ethoxycarbonothioyl)thio)propanoate, poly(3-methyl-*N*-vinylcaprolactam), *N*-vinylpyrrolidone monomer, and PMVC$_{58}$-*b*-PVPON$_{65}$ diblock copolymer. AFM topography images of PMVC$_{58}$-*b*-PVPON$_{65}$ diblock copolymer vesicles exposed to 25 °C and 4 °C for 12 hours. See DOI: https://doi.org/10.1039/d4ma00831f

‡ V. K. and Y. Y. equally contributed to this work.

shapes,[9–12] long-term solution stability, and adaptable physicochemical properties due to diverse chemistry of polymers.[13–15] The vesicle morphology can be considered advantageous over micelles or other nano-vehicles due to its ability to encase both hydrophilic (within its interior cavity) and hydrophobic (within the hydrophobic membrane) payloads and maintain the cargo for periods of months due to less fluid structures, unlike liposomes.[16] Amphiphilic block copolymers generally assemble into vesicles when the hydrophilic-to-total mass ratio is within 35 ± 10% for copolymer molecular weights in the range from 2700 to 20 000 g $mol^{-1}$.[9,16,17] As a general rule, increasing the molecular weight of the hydrophilic block within this ratio leads to a nanovesicle size decrease.[9,16]

Two main assembly approaches are used for copolymer assembly into vesicles, including solvent-switching (or nanoprecipitation) and thin-film rehydration, where organic solvents are used to dissolve copolymers.[2,18] During the nanoprecipitation approach, either another organic solvent (or water) is added to induce nano-aggregation of hydrophobic blocks in solution, which form the inner part of the vesicle membrane, while the hydrophilic blocks create the hydrophilic corona of the vesicle membrane. For example, we demonstrated that biocompatible poly(*N*-vinylcaprolactam)-*b*-poly(dimethylsiloxane)-*b*-poly(*N*-vinylcaprolactam) (PVCL-*b*-PDMS-*b*-PVCL) amphiphilic triblock copolymers could assemble *via* nanoprecipitation into nano-sized polymer vesicles (<200 nm) that encapsulated small anticancer drug doxorubicine (DOX) with no leakage at pH = 7 and 25 °C for at least a month and showed no toxicity *in vivo*.[19–21] The solvent-switching method can also be used in various modes,[2] including microfluidic mixing, which allows for rapid formation of both small (<300 nm) and giant unilamellar vesicles (≥1 μm).[22,23] Using microfluidic mixing, we showed the formation of giant unilamellar vesicles of a micrometer size (1.4 ± 0.2 μm) from both PVCL-*b*-PDMS-*b*-PVCL and poly(*N*-vinylpyrrolidone)-*b*-PDMS-*b*-poly(*N*-vinylpryrrolidone) (PVPON-*b*-PDMS-*b*-PVPON) triblock copolymers dissolved in ethanol and mixed with water.[24]

In the thin-film rehydration approach, a thin layer of a copolymer is first formed when the organic solvent evaporates, which is then hydrated upon adding aqueous media, forming polymer vesicles. We used this approach to obtain PVPON-*b*-PDMS-*b*-PVPON triblock copolymer vesicles to deliver PARP1 siRNA to breast cancers *in vivo*.[25] In both methods, additional purification from organic solvents *via* dialysis may be necessary, while in the rehydration method, long sonication and stirring are generally necessary to induce vesicle assembly.[18] In addition, film rehydration generally results in multilamellar vesicles that need to go through several cycles of sonication and extrusion to obtain true unilamellar structures, which can be time-consuming and may affect properties of encapsulated cargos, especially biomolecules.[2,16,18]

All-aqueous assembly of polymer vesicles can be beneficial for developing encapsulation and controlled release technologies of biological molecules and promoting clinical translation of therapeutic proteins, peptides, and nucleic acids. In this case, the development of stimuli-sensitive copolymers able to acquire amphiphilicity in response to changes in pH or temperature becomes crucial.[26] For example, a zwitterionic diblock copolymer of two polypeptide blocks poly(L-glutamic acid)-*b*-poly(L-lysine) soluble in aqueous solution at neutral pH in the range of 5 < pH < 9, produced polymer vesicles at highly acidic (pH < 4) or basic (pH > 10) conditions.[27] Conversely, a biocompatible zwitterionic copolymer, poly[2-(methacryloyloxy)ethyl phosphorylcholine]-*b*-poly[2-(diisopropylamino)ethyl methacrylate] showed spontaneous vesicle formation in aqueous solution when solution acidity was switched from pH = 2 to pH > 6 due to the deprotonation of the amine groups.[28] Often, the vesicle membrane obtained from the pH-sensitive copolymers must be crosslinked to ensure its integrity under physiological conditions.

Changing solution temperature to induce copolymer amphiphilicity has been useful in obtaining polymer vesicles from block copolymers with temperature-sensitive polymer blocks with either lower critical solution temperature (LCST) or upper critical solution temperature (UCST).[29] The LCST polymer blocks are soluble in water below the LCST and exhibit a coil-to-globule transition above that that can lead to the formation of self-assembled vesicles upon heating.[30–33] Poly(*N*-isopropylacrylamide) (PNIPAM), a well-studied LCST polymer with a coil-to-globule phase transition above 32 °C, was shown to obtain copolymers hydrophilic at room temperature that could assemble into vesicles at $T > 32$ °C.[34,35] For example, poly(ethylene oxide)-*b*-PNIPAM (PEO-*b*-PNIPAM) diblock copolymers formed stable polymer vesicles at $T \geq 37$ °C when the weight fraction of the hydrophilic block was less than 21%.[30] When using poly(*N*-(3-aminopropyl)methacrylamide hydrochloride) as a block for PNIPAM-based copolymer, stable copolymer vesicles were observed at $T > 45$ °C.[32] Temperature-sensitive poly(2-(dimethylamino)ethyl methacrylate) was also used to obtain block copolymers hydrophilic at 25 °C that assembled into vesicles at 39 °C but at an extreme solution pH of 11.[36] Hence, higher than physiological temperatures were shown to be essential to form and maintain the integrity of the PNIPAM-based temperature-responsive vesicles. In addition, PNIPAM was shown to induce systemic toxicity and release toxic small molecules upon hydrolysis in biological conditions and might not be well suited for biomedical applications.[37–40]

PVCL is an LCST polymer with superior biocompatibility and non-toxicity and a coil-to-globule transition near the body temperature that was used to produce a wide variety of temperature-sensitive copolymers and nanoscale materials.[41,42] Unlike PNIPAM, PVCL's phase transition occurs without intrachain hydrogen bonding and the polymer starts repelling water molecules at 30 °C, continuing up to 50 °C when PVCL entirely collapses and squeezes out the water molecules.[41] For example, while $PVCL_{155}$ homopolymer obtained *via* reversible addition–fragmentation transfer polymerization (RAFT) had the LCST = 39 °C, its diblock copolymer with PVPON, $PVCL_{155}$-*b*-$PVPON_{164}$ could assemble into polymer vesicles at a higher temperature of 42.5 °C[43] and their vesicle morphology could stabilize through intermolecular hydrogen bonding between PVPON corona and tannic acid.[44] Earlier, we showed that PVCL-*b*-PDMS-*b*-PVCL

polymersomes assembled *via* nanoprecipitation were stable at room temperature and would reversibly shrink between 25 °C and 45 °C due to enhanced hydrophobic interactions between PVCL chains without losing vesicle morphology.[19] The PVCL collapse at elevated temperatures resulted in the PDMS inner shell disturbance, which increased the shell permeability. The PVCL molecular weight could control the temperature range and the amount of DOX released from those vesicles.[19]

We also showed that besides molecular weight and concentration,[45] PVCL phase transition temperature can be modulated by increasing PVCL's hydrophobicity. For instance, VCL monomer methylation at α-position to produce 3-methyl-*N*-vinylcaprolactam (MVC) monomer brought the corresponding PMVC homopolyme's phase transition close to 0 °C. The MVC-based block copolymers, poly(MVC-*co*-VCL)-*b*-(VCL-*co*-VPON), demonstrated two LCST transitions from 19 to 42 °C.[46] Earlier, we synthesized $PMVC_{58}$-*b*-$PVPON_m$ ($m$ = 65, 98) diblock copolymers that were water-soluble below 14–20 °C and existed as polymer vesicles at 25–37 °C.[47] Increasing the PVPON length from 20 to 65 and 98 monomer units increased the copolymer's LCST from 15.2, 18.6, and 19.2 °C, respectively.[47] In addition, $PMVC_{58}$-*b*-$PVPON_{65}$ polymersomes displayed good stability in serum because of high PVPON hydrophilicity, which helps prevent protein adsorption. The $PMVC_{58}$-*b*-$PVPON_{65}$ polymersomes could entrap DOX with high encapsulation efficiency (95%) and loading capacity (49%) and did not cause any mortality in mice.[47]

In this work, we explored the temperature-sensitive behavior of $PMVC_{58}$-*b*-$PVPON_{65}$ to understand what intermediate structures could exist in the temperature range from 37 to 4 °C and the possible effects of lower temperatures on the vesicle size and shell thickness. We hypothesized that the $PMVC_{58}$-*b*-$PVPON_{65}$ hydrophilicity ratio (45%) will gradually decrease upon the temperature drop, and the copolymer morphology may gradually change. We employed dynamic light scattering (DLS), atomic force microscopy (AFM), transmission electron microscopy (TEM), and small-angle neutron scattering (SANS) to investigate the vesicle structure in solution at 4 °C $\leq T \leq$ 37 °C. SANS analysis was used to follow a gradual structure evolution at 37–4 °C. We examined the hydration of the vesicle shell using the SANS contrast matching technique, where the gradually decreased volume of $D_2O$ in $D_2O/H_2O$ mixtures was employed to observe the difference between the scattering length density (SLD) from the vesicle membrane and the solvent SLD due to an influx of solvent within the copolymer membrane. We correlated the shell hydration observed with SANS with the release of Alexa Fluor 488 fluorescent dye encapsulated into $PMVC_{58}$-*b*-$PVPON_{65}$ vesicles at 37–14 °C. Our study provides new fundamental insights on temperature-sensitive polymer vesicles and demonstrates a facile temperature-triggered approach for an all-aqueous assembly of copolymer vesicles stable at 20–37 °C that can be highly desirable for encapsulating a wide range of biological molecules, including proteins, peptides, and nucleic acids into stable polymer vesicles without a need of organic solvents. In addition, our findings could play a vital role in advancing encapsulation and controlled-release technologies aimed at managing oxidative stress in agricultural crops caused by low temperatures.[48]

## 2. Experimental section

### 2.1 Materials

2,2′-Azobis(2-methylpropionitrile) (AIBN) was purchased from Sigma-Aldrich, recrystallized from methanol, and dried in a vacuum at room temperature before use. *N*-Vinylcaprolactam (VCL) and *N*-vinylpyrrolidone (VPON) were purchased from Sigma-Aldrich and purified by vacuum distillation (*ca.* 1.5 torr) before reactions. 1,4-Dioxane, tetrahydrofuran (THF), and diisopropylamine (DIPA) were from Sigma-Aldrich and were freshly distilled before use. Hexane, methyl iodide ($CH_3I$), dichloromethane, methanol, *n*-butyllithium (2.5 M *n*-butyllithium solution in hexane), and methyl-2-bromopropionate were purchased from Fisher and used as received. Linear polystyrene standards for gel permeation chromatography (GPC) analysis were purchased from Agilent. Deionized water (DI) with a resistivity of 18.2 Ω cm was used for aqueous solutions.

### 2.2 RAFT Synthesis of PMVC macroinitiator and $PMVC_{58}$-*b*-$PVPON_{65}$ diblock copolymer

$PMVC_{58}$-*b*-$PVPON_{65}$ diblock copolymer used in this study was obtained previously by sequential copolymerization of 3-methyl-*N*-vinylcaprolactam (MVC) and *N*-vinylpyrrolidone (VPON) using methyl 2-((ethoxycarbonothioyl)thio)propanoate as a RAFT chain transfer agent (CTA).[47] Briefly, the CTA was prepared as described previously.[43] *O*-Ethyl xanthic acid potassium salt (5.6 g, 35 mmol) suspension in 10 mL of methanol was added dropwise to methyl-2-bromopropionate (5.0 g, 30 mmol) in 40 mL of methanol on an ice bath. After 24 h, the reaction mixture was filtered (to remove KBr) and extracted with a hexane/ethyl ether mixture (200 mL, 1 : 1, v/v), followed by drying on a rotary evaporator and further purification using column chromatography (acros organics, 0.035–0.070 mm particle size, 60 Å pore size) with chloroform : hexane eluent (3 : 2 v/v), concentrated in the rotary evaporator and dried in the vacuum (<1 mm Hg) for 24 hours at room temperature.

To obtain MVC monomer,[46] a 50 mL Schlenk reactor with a magnet stirring bar was charged with freshly distilled 2.02 g (0.02 mol) of diisopropylamine and 8.0 mL of anhydrous THF. The solution was stirred in the ice bath (0 °C) and under an argon (AirGas) atmosphere for 15 min. Then, 8.0 mL of 2.5 M *n*-butyllithium solution in hexane (0.02 mol) was added dropwise (1–2 minutes), followed by stirring for 10–15 minutes. After that, the mixture was cooled to −78 °C in a dry ice bath and stirred for 10–15 minutes. The solution of VCL (2.78 g, 0.02 mol) in 8.0 mL of anhydrous THF was added dropwise (1–2 minutes) to the mixture, and the resulting solution was maintained at −78 °C for 30 min. Finally, 2.8 g of $CH_3I$ (0.02 mol) in 8.0 mL anhydrous THF was added dropwise to the solution at −78 °C (1–2 minutes) in a dry ice bath and stirred for an additional 2 hours at −78 °C. Then, the resulting

mixture was poured into diethyl ether and separated from the aqueous phase. The ether layer was rinsed with water, and then the organic solution was concentrated on a rotary evaporator and purified by column chromatography on silica gel (acros organics, 0.035–0.070 mm particle size, 60 Å pore size) with ethyl acetate : hexane (1 : 20, v/v) as eluent. The desired fractions were combined, concentrated by a rotary evaporator, and dried in a vacuum at room temperature, yielding MVC as a colorless oil (yield: 2.56 g, 83%). We described the RAFT polymerization of MVC in our earlier works.[46,47] Briefly, MVC monomer, AIBN, and 1,4-dioxane were mixed with the CTA in a Schlenk flask ($[M]_0/[CTA]$ ratio = 540/1 and the [CTA]/[I] ratio = 2.3/1) followed by three cycles of freeze–pump–thaw under argon. The mixture was heated for 6 hours at 60 °C, and the polymerization was quenched in a dry ice bath. The obtained PMVC-CTA macroinitiator (yield 75%) had $M_n$ = 8900 g mol$^{-1}$, $M_w$ = 10 000 g mol$^{-1}$, $Đ$ = 1.12 as per calibration using linear polystyrene in THF (Agilent).[46] After that, the macroinitiator was mixed with VPON monomer in 1,4-dioxane solution, and after three cycles of freeze–pump–thaw degassing, the mixture was polymerized at 60 °C for 5 hours (28% conversion).[47] The copolymer was purified by precipitation in hexane two times, dried in a vacuum, and dialyzed at ≤10 °C in DI water (MWCO 6–8 kDa, Spectrum Spectra/Por) to convert RAFT end moieties to hydroxyl end-groups,[25,44] and freeze-dried. The number-average molecular weight obtained from $^1$H NMR analysis was 16 200 g mol$^{-1}$ ($M_n$ 9900 g mol$^{-1}$, $Đ$ = 1.14 from GPC analysis).[47]

### 2.3 Assembly of $PMVC_{50}$-*b*-$PVPON_{60}$ polymersomes

The self-assembly of $PMVC_{58}$-*b*-$PVPON_{65}$ diblock copolymer in water was carried out by mixing the copolymer (5 mg) with DI water (2 mL) followed by cooling the mixture in a freezer at 4 °C for 20 minutes. After cooling, the solution was brought to room temperature (25 °C), sonicated on the water bath, and then dialyzed against 0.01 M phosphate buffer (pH = 7.2) for 48 hours (MWCO 20 kDa, Fisher Scientific). For assembly of polymersomes in deuterium oxide ($D_2O$; Cambridge Isotope Laboratories, Inc.), $PMVC_{58}$-*b*-$PVPON_{65}$ copolymer (3 mg) and $D_2O$ (1 mL) were mixed and cooled at 4 °C for 20 minutes, and the solution was brought to a room temperature (25 °C) for the copolymer self-assembly. Before neutron scattering measurements, the sample was diluted with $D_2O$ to 1 mg mL$^{-1}$ followed by vertexing.

### 2.4 Electron transmission microscopy (TEM)

TEM images of the $PMVC_{58}$-*b*-$PVPON_{65}$ polymersomes were collected with a FEI Tecnai T12 Spirit TWIN TEM microscope operated at 80 kV. For sample preparation, the polymersome solutions were equilibrated at 37, 25, 14, and 4 °C. Specifically, the polymersomes prepared at 25 °C were incubated in an incubator at 37 °C or at 14 °C for 12 hours to obtain the sample at 37 °C and 14 °C, respectively. The sample at 4 °C was prepared from the polymersomes obtained at 25 °C and further incubated in a cold room at 4 °C for 12 hours. TEM grids, uranyl acetate solution (1%), and transfer pipettes were also incubated at a desired temperature before use. For analysis, 7 μL of a polymersome solution was dropped onto a Formavar/Carbon-coated copper grid (200 mesh, TED Pella), and the excess solution was blotted off of the bottom of the grid after 60 s with Kimwipe paper at a corresponding temperature. All polymersome samples prepared for TEM were stained with uranyl acetate for 10 seconds.

### 2.5 Dynamic light scattering (DLS)

Hydrodynamic size measurements of the polymersomes were obtained from three independent measurements of aqueous copolymer polymer solutions (2.5 mg mL$^{-1}$) at a desired temperature using a Nano-ZS Zetasizer (Malvern) equipped with He–Ne laser (663 nm). The average hydrodynamic size was acquired by peak fitting the intensity *versus* size curves using Origin Pro 2023 software, with the size standard deviation defined as the full width at half maximum.

### 2.6 Atomic force microscopy (AFM)

Topography images from $PMVC_{58}$-*b*-$PVPON_{65}$ polymersomes were collected using an NT-MDT AFM in tapping mode in the air. Scanning was performed using NSG30 probes (typical tip curvature radius = 6 nm, force constant = 22–100 N m$^{-1}$, and resonance frequency = 240–440 kHz) at 0.8 Hz scan rate. Polymersome samples prepared for TEM imaging were directly mounted on the AFM platform for imaging. The particle height was analyzed using AFM section analysis.

### 2.7 Small-angle neutron scattering (SANS)

SANS measurements were performed with the EQ-SANS instrument at the Spallation Neutron Source (SNS, BL-6) and Bio-SANS at High Flux Isotope Reactor (HFIR, CG-3) at Oak Ridge National Laboratory (USA).[49] To cover the $q$-range needed, instrument configurations with a sample-to-detector distance of 4 m (wavelength ∼10–13 Å) with an instrument chopper setting at 60 Hz were used. The sample aperture was set to 10 mm in diameter. The measurements were carried out using 600 μL of a sample in a 2-mm Banjo cell. A water bath controlled the sample temperature. The neutron wavelengths were converted from the time-of-flight and then were used to reduce data into reciprocal $q$ space, where $q = 4\pi \sin(\theta)/\lambda$; $2\theta$ is the scattering angle, and $\lambda$ is the neutron wavelength. The conversion and other reduction procedures, such as normalization for incident flux spectrum, sample transmission, detector sensitivity, the detector dark current, and azimuthal average, were performed with the facility-provided data reduction software Mantid. NIST SANS data analysis packages in Igor Pro[50] were used for data analysis. Fit quality was determined by minimizing the goodness-of-fit parameter ($\chi^2$), and parameters were constrained to physically reasonable values of size and thickness with consistency with DLS and TEM analyses.

The data was quantitatively analyzed by performing a modified Guinier analysis.[51,52] At larger $q$, corresponding to smaller length scales, where the thickness is much smaller than the overall size of the polymersome, the curvature of the

polymersome becomes unimportant; instead, it can be viewed as a sheet with a thickness $d$. For $qR_g < 1$, where $R_g$ is related to the thickness as $d = R_g\,(12)^{1/2}$, the intensity of scattering from a sheet goes as

$$I(q) \propto \frac{1}{q^2} e^{-q^2 R_g^2} \quad (1)$$

Therefore, from fitting $\ln(I(q)q^2)$ *versus* $q^2$, $R_g{}^2$ can be derived from the slope from which the thickness can be calculated.

The Guinier–Porod model was applied to obtain the overall size, $R_{g1}$, of the polymersomes.[53] The scattering intensity $I(q)$ is given as

$$I(q) = I_0 e^{-\frac{q^2 R_{g1}{}^2}{3-s}} \quad (2)$$

where $R_{g1}$ is the radius of gyration of the particles, and $s$ is the dimension variance.

### 2.8 Contrast matching SANS measurements

$H_2O/D_2O$ mixtures were prepared using DI $H_2O$ with 0, 20, 40, and 80 vol% of $H_2O$. $PMVC_{58}$-*b*-$PVPON_{65}$ copolymer was dissolved in $D_2O/H_2O$ solutions at 3 mg $mL^{-1}$, followed by solution cooling at 4 °C for 30 minutes and sonicating in the water bath at room temperature for the copolymer self-assembly. Before SANS measurements, the samples were diluted to 1 mg $mL^{-1}$ and vortexed. The samples were equilibrated for at least four hours for each temperature measurement. The samples were first measured at 25 and 37 °C and then cooled from 37 °C to 14 °C and to 4 °C using dry nitrogen purging to prevent vapor condensation for the measurements at lower temperatures.

### 2.9 Encapsulation and release of small molecules from $PMVC_{58}$-*b*-$PVPON_{65}$ vesicles at varied temperatures

The temperature-dependent release of a small molecular weight fluorescent dye from $PMVC_{58}$-*b*-$PVPON_{65}$ polymersomes was explored using Alexa Fluor 488 succinimidyl ester fluorescent dye (ThermoFisher). For the dye loading, $PMVC_{58}$-*b*-$PVPON_{65}$ (10 mg) was dissolved in 5 mL of the dye aqueous solution (0.4 mg $mL^{-1}$) in a fridge (4 °C) followed by incubation at 37 °C. The free non-encapsulated dye was removed from the Alexa-vesicle solution by dialysis using a 20 KDa MWCO float-a-lyzer at 37 °C in the incubator. The dye was released *via* dialysis of purified Alexa-loaded polymersomes in a 20 KDa MWCO float-a-lyzer at 37, 25, and 14 °C. Dialysis water was changed daily, and the fluorescence intensity of the polymersome solution was characterized by a fluorometer (Varian Cary). Relative fluorescence intensity was calculated by the ratio of the final fluorescence intensity in solution after its dialysis at a desired temperature and the initial fluorescence intensity (obtained after dialysis of the encapsulated dye sample at 37 °C) multiplied by 100.

## 3. Results and discussion

### 3.1 All-aqueous assembly of $PMVC_{58}$-*b*-$PVPON_{65}$ diblock copolymer

This study used $PMVC_{58}$-*b*-$PVPON_{65}$ diblock copolymer obtained earlier using RAFT polymerization.[47] The three-step synthesis approach is first based on methylation of VCL ring using *n*-BuLi/$CH_3I$ in THF to obtain methylated VCL monomer (MVC) (Fig. 1(a) and Fig. S1, ESI†) which can be then polymerized *via* RAFT using methyl 2-((ethoxycarbonothioyl)thio)propanoate as a RAFT chain transfer agent (CTA, Fig. S2, ESI†) in 1,4-dioxane to result in PMVC microinitiator (Fig. 1(b) and Fig. S3, ESI†). The PMVC macro-CTA can further participate in copolymerization with VPON (Fig. S4, ESI†) monomer in 1,4-dioxane at 60 °C resulting in the $PMVC_n$-*b*-$PVPON_m$ diblock copolymers (Fig. 1(c) and Fig. S5, ESI†). As reported earlier, aqueous dialysis of PVPON homopolymers synthesized *via* RAFT using methyl *O*-ethyl-*S*-(1-methoxycarbonyl)ethyl dithiocarbonate leads to the loss of the active CTA end-group through hydrolysis leaving behind hydroxyl end-group at the PVPON block end.[25,54]

In our previous study, the temperature-dependent optical density analysis of $PMVC_{58}$-*b*-$PVPON_{65}$ diblock copolymer solution revealed the onset of the copolymer's phase change associated with the coil-to-globule transition starting at ~14 °C with a continuous increase of the optical density up to ~23 °C which then plateaued.[47] Using cryo-TEM and SANS analysis, the copolymer was found to self-assemble into unilamellar polymer

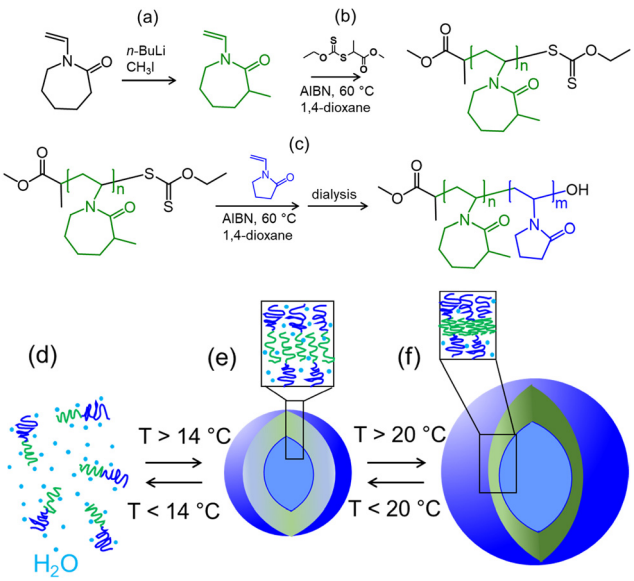


Fig. 1 The $PMVC_{58}$-*b*-$PVPON_{65}$ diblock copolymer is synthesized using a three-step approach: (a) synthesis of 3-methyl-*N*-vinylcaprolactam monomer (MVC), and (b) RAFT polymerization of MVC monomer to obtain $PMVC_{58}$ macroinitiator followed by (c) RAFT copolymerization of VPON monomer starting from the $PMVC_{58}$ macroinitiator to obtain the $PVPON_{65}$ block. The $PMVC_{58}$-*b*-$PVPON_{65}$ diblock copolymer was assembled into vesicles by first dissolution in water at low temperature, $T \leq 10$ °C (d), until its molecular dissolution, followed by the solution incubation at $T > 20$ °C (e) and (f).

vesicles which were stable at room temperature (20–25 °C) for at least 50 days as measured using DLS.[47] In the current work, the vesicle assembly from $PMVC_{58}$-*b*-$PVPON_{65}$ was carried out by its dissolution in DI water at a low temperature (4–10 °C) for 20 minutes until solution transparency (Fig. 1(d)), followed by sonication in a water bath to ensure a uniform temperature throughout the solution. After the molecular dissolution of the copolymer, the solution was brought to 25 °C using an incubator and dialyzed for 48 hours in water to trigger copolymer self-assembly and to purify the obtained polymer vesicles (Fig. 1(e) and (f)).

The polymersome solutions were equilibrated at 37 °C, 25 °C, 14 °C, and 4 °C in an incubator to understand changes in the morphology of the $PMVC_{58}$-*b*-$PVPON_{65}$ copolymer assemblies upon lowering the solution temperature. For that, the polymersomes prepared at 25 °C were incubated at 37 °C or 14 °C for 12 hours to obtain the vesicle samples at 37 °C and 14 °C, respectively. The vesicle sample at 4 °C was prepared by incubating the polymersomes obtained at 25 °C in a cold room at 4 °C for 12 hours. TEM analysis of the vesicles revealed that all samples, except the one at 4 °C, maintained their initial vesicle morphology with spherically shaped vesicles distinctively visible at the scale of 200 nm (Fig. 2(a)–(c)). In contrast, the sample prepared at the lowest temperature (4 °C) did not show any structures of a similar shape and size (Fig. 2(d)).

Conversely, much smaller nanoassemblies could be seen in the TEM image for the 4 °C-copolymer sample with an average dry size of 15 ± 5 nm. Given its molecular weight, the copolymer chain $R_g$ was estimated to be 3 nm, which may indicate that the copolymer vesicles could dissociate into molecular chains or chain aggregates at 4 °C. Indeed, the section analysis of the AFM topography images of the vesicles dried on the TEM grids showed that the particle height was 35 ± 5 nm for the polymersomes at 25 °C (Fig. S6a, ESI†), while it was 3.5 ± 0.3 nm (Fig. S6b, ESI†) for the sample exposed to a lower temperature of 4 °C, which agrees with the TEM data and the copolymer $R_g$ estimation at the lowest temperature.

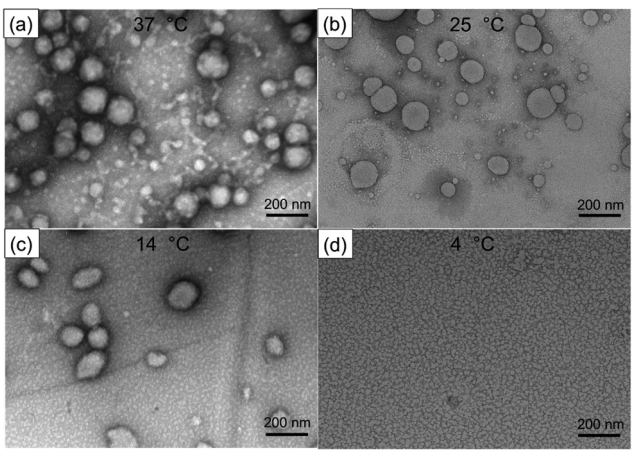


Fig. 2 TEM images of $PMVC_{58}$-*b*-$PVPON_{65}$ polymersomes dried on TEM grids from solutions at (a) 37 °C, (b) 25 °C, (c) 14 °C, and (d) 4 °C.

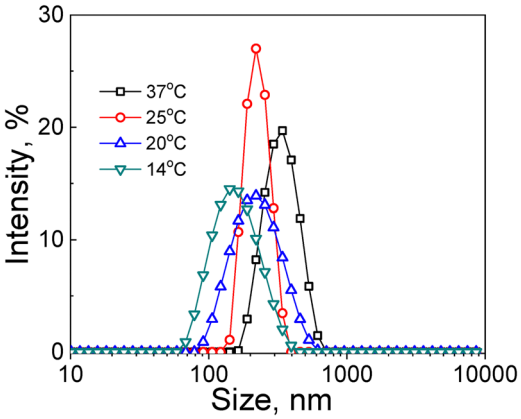


Fig. 3 The hydrodynamic size of $PMVC_{58}$-*b*-$PVPON_{65}$ copolymer vesicles analyzed in solutions at 37 °C (black squares), (b) 25 °C (red circles), (c) 14 °C (blue up-triangles), and (d) 4 °C (green down-triangles) as measured by DLS.

On the other hand, the AFM height of the vesicles at 25 °C corresponds to a double-shell thickness of the $PMVC_{58}$-*b*-$PVPON_{65}$ polymersome, which gives the vesicle single shell a thickness of ~17.5 nm. This result is in excellent agreement with the $PMVC_{58}$-*b*-$PVPON_{65}$ vesicle shell thickness of 17.7 ± 2.2 nm as measured by SANS and reported previously.[47] This AFM result also indicates that the vesicles prepared at 25 °C acquired a flattened shape upon drying while keeping their overall integrity, and the double-shell thickness of 35 nm agrees with the unilamellar structure of the $PMVC_{58}$-*b*-$PVPON_{65}$ vesicles.

Along with vesicle disassembly at $T < 14$ °C, lowering the solution temperature affected the polymer vesicle size in the range of 14 °C < $T$ < 37 °C. DLS analysis revealed that the average hydrodynamic diameter of the vesicles gradually decreased from 350 ± 150 nm at 37 °C (Fig. 3, black squares, Table 1) to 240 ± 94 nm (Fig. 3, red circles, Table 1) and 230 ± 48 nm (Fig. 3, blue up-triangles, Table 1) at 25 °C and 20 °C, respectively. Moreover, almost a two-fold decrease in the vesicle hydrodynamic size from 350 ± 190 nm to 142 ± 50 nm was observed when the solution temperature was decreased from 37 to 14 °C (Fig. 3, green down-triangles, Table 1).

The gradual decrease of the vesicle size as measured by DLS could indicate the increasing hydrophilicity of the inner shell of the vesicles, resulting in gradual PMVC block stretching due to chain uncoiling in the 14 °C < $T$ < 37 °C. The release of molecular chains from the assembled vesicle may result from such increased hydrophilicity of the PMVC inner layer of the vesicle shell, leading to the size decrease observed in DLS measurements. We analyzed the vesicles in solutions at gradually lowered temperatures using SANS to study the changes in the vesicle size and shell thickness.

### 3.2 SANS analysis of $PMVC_{58}$-*b*-$PVPON_{65}$ copolymer vesicles in solutions at varied temperatures

The SANS analysis of $PMVC_{58}$-*b*-$PVPON_{65}$ copolymer vesicles in solutions was carried out at 37, 25, 20, 14, and 4 °C. The

Table 1 Hydrodynamic diameter (nm) of $PMVC_{58}$-*b*-$PVPON_{65}$ vesicles in solutions exposed to varied temperatures (°C) as measured by DLS

| Solution temperature, °C | 37 | 25 | 20 | 14 |
|---|---|---|---|---|
| Hydrodynamic diameter, nm | 350 ± 190 | 240 ± 94 | 230 ± 48 | 142 ± 50 |

copolymer assembly was done by dissolving the polymer in $D_2O$ at ~4 °C followed by solution incubation at 37 °C. Further measurements were continued by cooling the sample to 25, 20, 14, and 4 °C with at least 4 hours of incubation for sample equilibration before neutron scattering measurements. We used the Guinier–Porod model to calculate the particle radius of gyration ($R_g$) at each temperature (Fig. 4). For all SANS plots, the dimension variance value, which can be used to distinguish between spherical, rodlike, or plate-like particle shape, was lower than 0.1, which being close to zero, describes a three-dimensional spherical shape of the particle.[53,55] Hence, the spherical shape of the $PMVC_{58}$-*b*-$PVPON_{65}$ copolymer assembly obtained by SANS was in good agreement with the TEM and AFM data for the $PMVC_{58}$-*b*-$PVPON_{65}$ copolymer vesicles at 37–14 °C. Furthermore, as temperature decreased from 37 to 4 °C, the intensity $I(0)$ at low $q$ region from the Guinier–Porod model fits decreased, while material concentration did not change. In addition, the curve shape at $I(0)$ with the lowest $q$ gradually became more flattened. These results also indicate a decrease in the particle size, especially at 4 °C, upon the temperature lowering (Fig. 4(a)–(e)).

The model fits in Fig. 4(a)–(e) resulted in $R_g$ values of 165 ± 8 nm, 123 ± 6 nm, 110 ± 6 nm, and 70 ± 4 nm at 37, 25, 20, and 14 °C, respectively, while that was 20.0 ± 0.5 nm for the sample

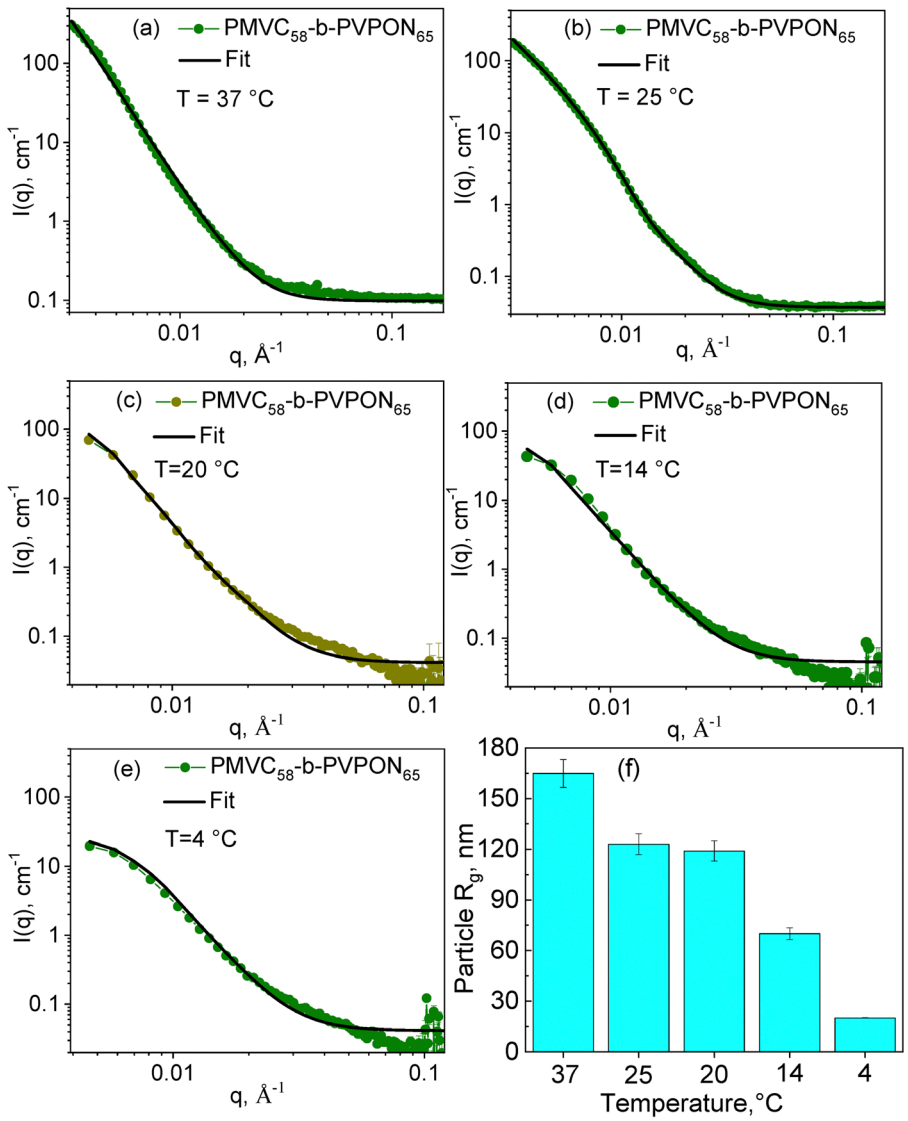


Fig. 4 SANS plots of the $PMVC_{58}$-*b*-$PVPON_{65}$ vesicle solutions and their Guinier fits (solid lines) at (a) 37 °C, (b) 25 °C, (c) 20 °C, (d) 14 °C, and (e) 4 °C. (f) The dependence of particle $R_g$ on solution temperature obtained from SANS plot fits (a)–(e).

Table 2 Particle $R_g$ (nm) and thickness of the vesicle shell (nm) in $PMVC_{58}$-*b*-$PVPON_{65}$ vesicle solutions at varied temperatures as measured by SANS

| Temperature, °C | 37 | 25 | 20 | 14 | 4 |
|---|---|---|---|---|---|
| Particle $R_g$, nm | 165 ± 8 | 123 ± 6 | 110 ± 6 | 70 ± 4 | 20.0 ± 0.5 |
| Shell thickness ($d$), nm | 17.6 ± 2.6 | 17.9 ± 2.1 | 22.4 ± 2.4 | 25.5 ± 5.8 | — |

exposed to 4 °C (Fig. 4(f) and Table 2). These $R_g$ data agree well with the hydrodynamic radii ($R_h$) calculated from the DLS data as $D_h/2 = R_h$ (Fig. 3 and Table 1), resulting in the ratio of $R_g/R_h$ of 0.943, 1.02, 0.957, and 0.986 for the sample at 37, 25, 20, and 14 °C, respectively. These values, being close to 1, indicate a hollow sphere with a non-negligable shell.[56] Hence, these results indicate that the $PMVC_{58}$-*b*-$PVPON_{65}$ copolymer vesicles maintain their vesicular morphology as an empty sphere with a non-negligible shell when the solution temperature is lowered from 37 to 14 °C

The $R_g$ for the sample at 4 °C was obtained from the SANS analysis to be 20.0 ± 0.5 nm (Fig. 4(f) and Table 2). Given that, for a solid sphere, the physical radius $R^2 = (5/3)\ R_g^2$,[55] the particle radius for the sample at 4 °C can be estimated as ~25 nm which is similar to the size of the particle obtained through the TEM analysis (15 ± 5 nm) (Fig. 2(d)). These results combined with the AFM height of the assembly (~3.5 nm) imply that the $PMVC_{58}$-*b*-$PVPON_{65}$ copolymer vesicles lose their vesicle morphology when exposed to 4 °C < $T$ < 14 °C and, most probably, exist as aggregates of a few copolymer chains due to decreased chain hydrophobicity.

To characterize temperature-induced changes in the vesicle shell in the temperature range 37 °C to 14 °C, the modified Guinier plots of the SANS data as $\ln I(q)\ q^2$ *versus* $q^2$ were obtained (Fig. 5) where the slope of a linear fit to the data produced $-R_g^2$ of the vesicle membrane from which the polymersome shell thickness, $d$, was calculated. The slopes of a linear fit to the data were found to be −2612 ± 158 Å$^2$, −2608 ± 145 Å$^2$, −4211± 132 Å$^2$, and −5438 ± 284 Å$^2$ for the vesicles at 37, 25, 20, and 14 °C, respectively. Hence, the vesicle shell thickness was calculated from the membrane $R_g$ values to be 17.6 ± 2.6 nm at 37 °C, 17.9 ± 2.1 nm at 25 °C, 22.4 ± 2.4 nm at 20 °C, and 25.5 ± 5.8 nm at 14 °C, respectively (Table 2).

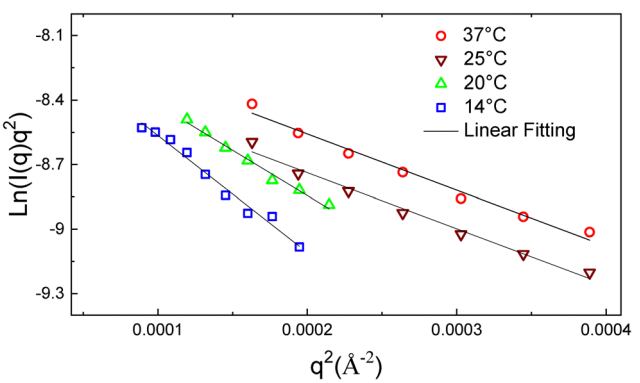


Fig. 5 Modified Guinier plots of $PMVC_{58}$-*b*-$PVPON_{65}$ copolymer vesicles and their linear fits at 37 °C (red circles), 25 °C (wine down-triangles), 20 °C (green up-triangles), and 14 °C (blue squares).

The $PMVC_{58}$-*b*-$PVPON_{65}$ vesicles thickness at 25 °C found by SANS analysis (17.9 ± 2.1 nm) agrees excellently with the double-shell thickness for these vesicles (35 ± 5 nm) obtained through the AFM analysis of the polymersomes dried from solution at this temperature (Fig. S6a, ESI†). Apparently, the increase in the polymersome shell thickness with decreasing temperature from 37 to 14 °C is mainly due to the gradually reducing hydrophobicity of PMVC under these conditions. In our earlier SANS study using PVCL-*b*-PDMS-*b*-PVCL triblock copolymer polymersomes, we observed the shrinkage of the polymer vesicle membrane when PVCL temperature-sensitive hydrophilic corona transited from a coil to a globule state upon temperature increase from 25 to 55 °C.[20] The temperature increase induced polymer vesicle size and shell thickness shrinkage by ~20% for those triblock copolymers depending on the ratio of the blocks in the copolymer.[20] Moreover, $PVCL_{10}$-*b*-$PDMS_{65}$-*b*-$PVCL_{10}$ polymersomes were found to become permeable to small molecules within 10 hours when temperature increased from 30 to 37 °C, releasing 20 and 70% of encapsulated DOX, respectively.[19] This behavior was rationalized through the PVCL phase change, resulting in the PVCL chains' collapse with subsequent polymersome shrinkage and local PDMS membrane disturbance by the collapsed PVCL chains, allowing the release of the small molecules from the vesicle interior.[19]

Conversely, we demonstrated previously that $PMVC_{58}$-*b*-$PVPON_{65}$ polymersomes with encapsulated DOX did not show any significant release of the drug (<5%) at 37 °C for at least 25 hours of observation. The exceptional stability of the shell towards a small molecule release at the physiological temperature was also demonstrated *in vivo* experiments with mice where drug-loaded $PMVC_{58}$-*b*-$PVPON_{65}$ polymersomes showed no cardiotoxicity compared to the free drug or liposome-loaded drug.[47] Our current SANS data demonstrate that the superior stability of the $PMVC_{58}$-*b*-$PVPON_{65}$ vesicles against drug release is due to the dense and compact vesicle shell at 37 °C while the vesicle thickness increases by 45% when the polymersomes are transferred from 37 to 14 °C implying the appearance a more loosely connected membrane with increased hydration (Table 2 and Fig. 1(e), (f)).

We employed the SANS contrast variation technique to observe possible polymersome hydration in response to a temperature decrease from 37 to 14 °C. Polymer vesicles as spheres with a hollow cavity can demonstrate a neutron contrast from the shell against $D_2O$, seen as the liquid 'core' and liquid exterior media in SANS. The coil-to-globule transition of PVCL observed earlier with SANS resulted in the dissociation of hydrogen bonds of the polymer with water and partial polymer dehydration, followed by a complete chain collapse upon water repulsion.[57] Increased hydration of $PMVC_{58}$-*b*-$PVPON_{65}$ vesicle

membrane in the temperature range from 25 to 14 °C can be expected as a result of an influx of solvent within the copolymer membrane; thus, the difference between the scattering length density (SLD) from the vesicle membrane and the solvent SLD is expected to decrease. We hypothesized that the vesicles exposed to a solvent mixture of $D_2O$ and $H_2O$ with decreasing amount of $D_2O$ from 80/20 to 20/80 ratio of $D_2O/H_2O$ solution, will be scattering differently at 37 °C unlike that at 14 °C with the scattering contrast decrease (or disappearance) at the lower temperature.

All $PMVC_{58}$-*b*-$PVPON_{65}$ vesicles showed strong scattering from good contrast at 37, 25, 20, and 14 °C in 100 vol% $D_2O$ (Fig. 4(a)–(d)). Fig. 6 demonstrates that the SANS plots ($I(q)$ *versus* $q$) showed enough scattering contrast for the samples at all four temperatures when the amount of $D_2O$ was decreased to 80% (Fig. 6(a)) or 60% (Fig. 6(b)) in the solvent mixture. From the estimated SLD for $PMVC_{58}$-*b*-$PVPON_{65}$ copolymer, its contrast matching point is about 18% $D_2O$. Hence, although with the decreased SLD due to increased shell hydration, the vesicles at 25–14 °C still exhibited considerate scattering contrast against the solvent mixtures with 80–60% $D_2O$.

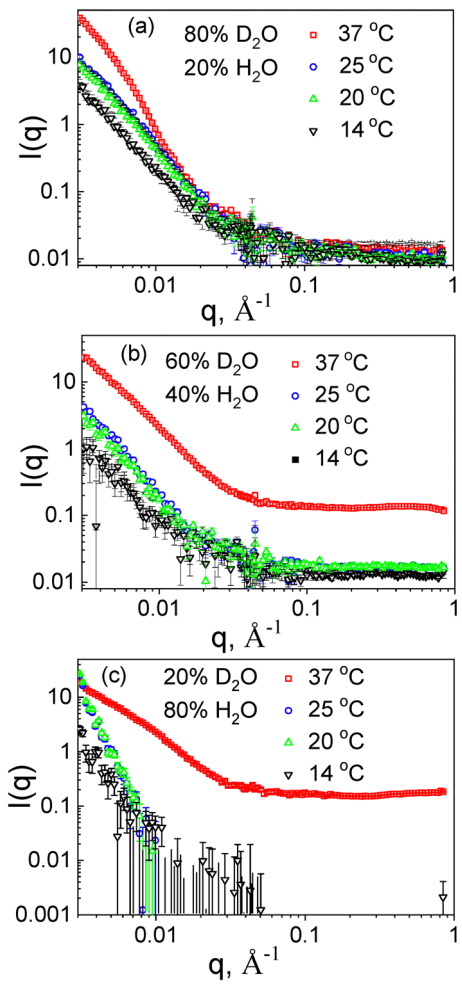


Fig. 6 Contrast-matching SANS plots of $PMVC_{58}$-*b*-$PVPON_{65}$ vesicles prepared in a solvent mixture of (a) 80/20% $D_2O/H_2O$, (b) 60/40% $D_2O/H_2O$, and (c) 20/80% $D_2O/H_2O$.

The vesicle hydration at lower temperatures is accompanied by the reformation of hydrogen bonds between $PMVC_{58}$ block and water, facilitating vesicle shell reswelling and the shell thickness increase due to the decrease in molecular density (Table 2). Fig. 6 demonstrates that the intensity drops significantly at 14 °C. This result indicates that more solvent penetrates the polymer vesicle shell (Fig. 1(e)), decreasing contrast and the scattering intensity decreases. The significant contrast loss happens for all studied contrasts due to an influx of solvent. At the 20% $D_2O$, the high degree of scattering contrast loss can be seen more obviously for the $PMVC_{58}$-*b*-$PVPON_{65}$ vesicles at 25, 20, and 14 °C (Fig. 6(c)) because the contrast to the solvent is much smaller, to begin with. Only the sample at 37 °C maintained its scattering pattern through all the contrasts, although with decreasing intensity.

The contrast-matching study results indicate that the hydration of the polymersome shell starts at temperatures below 20 °C (Fig. 1(e)). These findings agree with the earlier demonstrated excellent structure stability of the polymersomes at 25–37° and their retention of small molecular weight molecules under these conditions *in vivo*.[21]

### 3.3 Release of small molecules from $PMVC_{58}$-*b*-$PVPON_{65}$ vesicles at lower temperatures

To understand the release behavior from the $PMVC_{58}$-*b*-$PVPON_{65}$ polymersomes at lower temperatures and correlate this behavior with SANS data on polymer vesicle thickness, we encapsulated Alexa Fluor 488 fluorescent dye into the interior cavity of the vesicles and explored the dye release into solution at 37, 25, and 14 °C. For the dye loading, the $PMVC_{58}$-*b*-$PVPON_{65}$ copolymer was dissolved in a fridge in 5 mL of the dye aqueous solution (0.4 mg $mL^{-1}$), followed by the solution incubation at 37 °C. The non-encapsulated dye was removed from the Alexa-$PMVC_{58}$-*b*-$PVPON_{65}$ polymersome solution by dialysis at 37 °C in an incubator. The release of the dye was measured by analyzing the fluorescence intensity of the polymersome solution using fluorometry. The relative fluorescence intensity was calculated by the ratio of the final fluorescence intensity in solution at a desired temperature after dialysis, representing the amount of the dye left encapsulated inside the vesicle and the initial fluorescence intensity (the maximum encapsulated amount of the dye at 37 °C) multiplied by 100.

The fluorescence analysis showed that the relative fluorescence intensity from the polymersome solution did not significantly change after the solution temperature was decreased from 37 to 25 °C, with the corresponding intensity values being 97 ± 3% and 96 ± 3% (Fig. 7). This result demonstrates that despite a slight decrease in the vesicle size and negligible decrease in the vesicle thickness (Table 2) accompanied by little hydration (Fig. 6), no significant release of the dye can be induced, and the vesicles maintain their overall integrity securing the cargo inside.

In contrast, decreasing the solution temperature to 14 °C resulted in the 4.4-fold decrease in the relative fluorescence

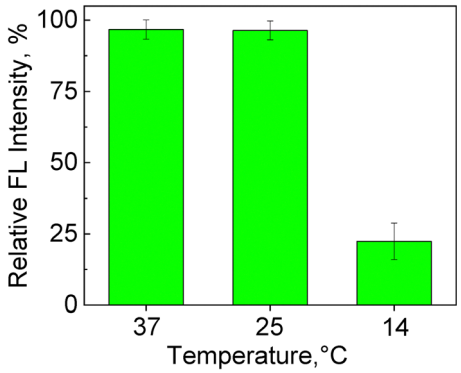


Fig. 7 Relative fluorescence (FL) intensity (%) from the Alexa Fluor 488-loaded $PMVC_{58}$-*b*-$PVPON_{65}$ polymersomes after their exposure to a desired temperature (37, 25, and 14 °C).

intensity with its final value of 22 ± 6% (Fig. 7). This result is in excellent agreement with the SANS data on the increased thickness of the vesicles and decreased neutron scattering due to the increased hydration of the vesicle shell at 14 °C (Fig. 6 and 1(e)). These combined data confirm our hypothesis about the loosened vesicle shell at $T \leq 14$ °C due to increased hydrophilicity of the $PMVC_{58}$-*b*-$PVPON_{65}$ copolymer as indicated by SANS contrast matching experiments (Fig. 6), allowing small hydrophilic dye molecules to diffuse through the vesicle shell accompanied by the vesicle rearrangement as indicated by decreased vesicle size (Fig. 3 and 4). Hence, the vesicle shell rearrangement induced by lowering the solution temperature below 14 °C facilitated the release of ~80% of the encapsulated dye, whereas less than 5% of the dye release was observed for the vesicle incubation at 37 and 25 °C (Fig. 7). The relatively quick release of the dye at 14 °C agrees with the increased vesicle thickness from 17.6 ± 2.6 nm (37 °C) to 25.5 ± 5.8 nm and increased hydration (decreased scattering) in contrast matching experiments (Fig. 6).

## 4. Conclusion

Herein, we explored the temperature-sensitive behavior of $PMVC_{58}$-*b*-$PVPON_{65}$ vesicles in response to lowering the solution temperature from 37 to 25, 20, 14, and 4 °C. The polymer vesicles were assembled from the diblock copolymer dissolved in aqueous solution at 4 °C and exposed to 25 °C. TEM analysis confirmed that the temperature lowering did not cause any loss in polymersome morphology in the temperature range from 37 to 14 °C. In contrast, no vesicles were observed at the lowest temperature of 4 °C. SANS analysis of the polymersome solutions at the varied temperatures confirmed the particle size decrease through the studied temperature range with model fitting resulting in a hollow sphere with a non-negligible shell in solutions at 37–14 °C. In contrast, the average vesicle thickness was found to increase from 17 nm at 37 °C to 25 nm at 14 °C with tighter and more uniform thickness at 37–25 °C and more loosened and expanded structure at 20–14 °C. From the SANS contrast matching study, this vesicle behavior is found to be driven by the gradual rehydration of the PMVC block at 37–14 °C. The demonstrated shell hydration at 20–14 °C was further correlated with the release of a fluorescent dye from the polymersomes upon temperature decrease. No significant (<5%) release of the dye was observed from the vesicles at 37–20 °C, with the corresponding intensity values being 97 ± 3% and 96 ± 3%, indicating that the polymersome membrane safely protected the encapsulated dye.

In contrast, decreasing the solution temperature to 14 °C resulted in a 4.4-fold decrease in the relative fluorescence intensity with its final value of 22 ± 6%, indicating ~80% of the dye release within 12 hours. Our SANS data, at temperatures 37 and 4 °C, show that the vesicles were stable at 37 °C for all 8 hours of the experiment. However, these vesicles were found to dissolve into molecular chains at 4 °C within four hours of sample equilibration (SANS). Our combined findings indicate the gradual structure evolution of $PMVC_{58}$-*b*-$PVPON_{65}$ copolymer vesicle from a dense-shell vesicle at 37–25 °C to a highly-hydrated shell vesicle at 20–14 °C to molecular chain aggregates at 4 °C. This work provides new fundamental insights into temperature-sensitive polymer vesicles by elucidating the delicate structure–property relationship between its constituents. Hence, the polymer vesicle assembly using temperatures below 14 °C from all-aqueous copolymer solutions instead of nanoprecipitation from organic solvents or solvent exchange can be highly desirable for encapsulating a wide range of biomolecules, including proteins, peptides, and nucleic acids into temperature-sensitive polymeric vesicles stable at physiologically relevant temperatures of 25–37 °C. This approach can further promote the clinical translation of therapeutic proteins and peptides and their controlled release. Furthermore, our findings can be crucial in developing encapsulation and controlled release technologies to regulate low-temperature induced oxidative stress in agriculture crops.

## Author contributions

V. K. – conceptualization, formal analysis, investigation, validation, visualization, writing – original draft, review & editing. Y. Y. – investigation, formal analysis, writing – original draft. S. Q. – data curation, formal analysis, resources, Writing – review/editing. E. K. – funding acquisition, conceptualization, project administration, resources, supervision, validation, writing – review & editing.

## Data availability

All the relevant data are available from the corresponding authors upon reasonable request.

## Conflicts of interest

There are no conflicts to declare.

## Acknowledgements

This work was funded by NSF DMR award #2208831. This material is partly based upon work supported under the IR/D Program by the National Science Foundation (E. K.). Any opinions, findings, conclusions, or recommendations expressed in this material are those of the author(s) and do not necessarily reflect the views of the National Science Foundation. UAB electron microscopy facility is acknowledged. Neutron scattering research used resources at HIFR and SNS, a DOE Office of Science User Facility operated by the Oak Ridge National Laboratory. The Bio-SANS instrument is supported by the Office of Biological and Environmental Research of the U.S. DOE. Dr Maksim Dolmat (UAB) is acknowledged for technical assistance with AFM. Dr Pavel Nikishau (UAB) is acknowledged for technical assistance with $^{1}$H NMR spectroscopy.

## References

1 S. G. Surapaneni, S. N. Choudhari, S. V. Avhad and A. V. Ambade, Permeable polymersomes from temperature and pH dual stimuli-responsive PVCL-*b*-PLL block copolymers for enhanced cell internalization and lysosome targeting, *Biomater. Adv.*, 2023, **151**, 213454.

2 Y. Zhu, B. Yang, S. Chen and J. Du, Polymer vesicles: Mechanism, preparation, application, and responsive behavior, *Prog. Polym. Sci.*, 2017, **64**, 1–22.

3 C. Turan, I. Terzioglu and I. Erel-Goktepe, Synthesis of Poly(2-isopropyl-2-oxazoline)-*b*-poly(2-phenyl-2-oxazoline)-*b*-poly(2-isopropyl-2-oxazoline) and its Self-assembly into Polymersomes: Temperature-Dependent Aqueous Solution Behaviour, *Mater. Today Commun.*, 2023, **35**, 106094.

4 J. F. Scheerstra, A. C. Wauters, J. Tel, L. K. E. A. Abdelmohsen and J. C. M. van Hest, Polymersomes as a potential platform for cancer immunotherapy, *Mater. Today Adv.*, 2022, **13**, 100203.

5 H. L. Che and J. C. M. van Hest, Stimuli-responsive polymersomes and nanoreactors, *J. Mater. Chem. B*, 2016, **4**, 4632–4647.

6 M. Li, C. Du, N. Guo, Y. Teng, X. Meng, H. Sun, S. Li, P. Yu and H. Galons, Composition design and medical application of liposomes, *Eur. J. Med. Chem.*, 2019, **164**, 640–653.

7 A. Jesorka and O. Orwar, Liposomes: technologies and analytical applications, *Annu. Rev. Anal. Chem.*, 2008, **1**, 801–832.

8 A. Himanshu, P. Sitasharan and A. K. Singhai, Liposomes as Drug Carriers, *Int. J. Pharm. Life Sci.*, 2011, **2**, 945–951.

9 P. L. Soo and A. Eisenberg, Preparation of Block Copolymer Vesicles in Solution, *J. Polym. Sci., Part B: Polym. Phys.*, 2004, **42**, 923–938.

10 R. Salva, J.-F. Le Meins, O. Sandre, A. Brulet, M. Schmutz, P. Guenoun and S. Lecommandoux, Polymersome Shape Transformation at the Nanoscale, *ACS Nano*, 2013, **7**, 9298–9311.

11 C. Huang, Y. Qin, S. Wu, Q. Yu, L. Mei, L. Zhang and D. Zhu, Temperature-Responsive ''Nano-to-Micro'' Transformed Polymersomes for Enhanced Ultrasound/Fluorescence Dual Imaging-Guided Tumor Phototherapy, *Nano Lett.*, 2024, **24**, 9561–9568.

12 C. K. Wong, M. H. Stenzel and P. Thordarson, Non-spherical polymersomes: formation and characterization, *Chem. Soc. Rev.*, 2019, **48**, 4019–4035.

13 Y. Zhu, S. Cao, M. Huo, J. C. M. van Hest and H. Che, Recent advances in permeable polymersomes: fabrication, responsiveness, and applications, *Chem. Sci.*, 2023, **14**, 7411–7437.

14 E. Rideau, R. Dimova, P. Schwille, F. R. Wurm and K. Landfester, Liposomes and olymersomes: a comparative review towards cell mimicking, *Chem. Soc. Rev.*, 2018, **47**, 8572–8610.

15 J. Lefley, C. Waldron and C. R. Becer, Macromolecular design and preparation of polymersomes, *Polym. Chem.*, 2020, **11**, 7124–7136.

16 D. E. Discher and A. Eisenberg, Polymer Vesicles, *Science*, 2002, **297**, 967–972.

17 H. Aranda-Espinoza, H. Bermudez, F. S. Bates and D. E. Discher, Electromechanical limits of polymersomes, *Phys. Rev. Lett.*, 2001, **87**, 208301.

18 C. Hua and L. Qiu, Polymersomes for Therapeutic Protein and Peptide Delivery: Towards Better Loading Properties, *Int. J. Nanomed.*, 2024, **19**, 2317–2340.

19 F. Liu, V. Kozlovskaya, S. Medipelli, B. Xue, F. Ahmad, M. Saeed, D. Cropek and E. Kharlampieva, Temperature-sensitive polymersomes for controlled delivery of anticancer drugs, *Chem. Mater.*, 2015, **27**, 7945–7956.

20 Y. Yang, A. Alford, V. Kozlovskaya, S. Zhao, H. Joshi, E. Kim, S. Qian, V. Urban, D. Cropek, A. Aksimentiev and E. Kharlampieva, Effect of Temperature ad Hydrophilic Ratio on the Structure of Poly(*N*-vinylcaprolactam)-*block*-poly(dimethylsiloxane)-*block*-poly(*N*-vinylcaprolactam) Polymersomes, *ACS Appl. Polym. Mater.*, 2019, **1**, 722–736.

21 V. Kozlovskaya, Y. Yang, F. Liu, K. Ingle, A. Ahmad, G. V. Halade and E. Kharlampieva, Dually Responsive Poly(*N*-vinylcaprolactam)-*b*-Poly(dimethylsiloxane)-*b*-Poly(*N*-vinylcaprolactam) Polymersomes for Controlled Delivery, *Molecules*, 2022, **27**, 3485.

22 A. Jahn, S. M. Stavis, J. S. Hong, W. N. Vreeland, D. L. DeVoe and M. Gaitan, Microfluidic mixing and the formation of nanoscale lipid vesicles, *ACS Nano*, 2010, **4**, 2077–2087.

23 S. Ota, S. Yoshizawa and S. Takeuchi, Microfluidic formation of monodisperse, cell- sized, and unilamellar vesicles, *Angew. Chem., Int. Ed.*, 2009, **48**, 6533–6537.

24 Y. Yang, V. Kozlovskaya, M. Dolmat, Y. Song, S. Qian, V. Urban, D. Cropek and E. Kharlampieva, Temperature Controlled Transformations of Giant Unilamellar Vesicles of Amphiphilic Triblock Copolymers Synthesized via Microfluididc Mixing, *Appl. Surf. Sci. Adv.*, 2021, **5**, 100101.

25 Y. Yang, V. Kozlovskaya, Z. Zhang, C. Xing, S. Zaharias, M. Dolmat, S. Qian, J. Zhang, J. M. Warram, E. S. Yang and E. Kharlampieva, Poly(*N*-vinylpyrrolidone)-*block*-poly(dimethylsiloxane)-*block*-poly(*N*-vinylpyrrolidone) Triblock Copolymer Polymersomes for Delivery of PARP1 siRNA to Breast Cancers, *ACS Appl. Bio Mater.*, 2022, **5**, 1670–1682.

26 S. S. Naik, J. G. Ray and D. A. Savin, Temperature- and pH-Responsive Self-assembly of Poly(propylene oxide)-*b*-Poly(lysine) Block Copolymers in Aqueous Solution, *Langmuir*, 2011, **27**, 7231–7240.
27 J. Rodrıguez-Hernandez and S. Lecommandoux, Reversible Inside-Out Micellization of pH-responsive and Water-Soluble Vesicles Based on Polypeptide Diblock Copolymers, *J. Am. Chem. Soc.*, 2005, **127**, 2026–2027.
28 J. Du, Y. Tang, A. L. Lewis and S. P. Armes, pH-Sensitive Vesicles Based on a Biocompatible Zwitterionic Diblock Copolymer, *J. Am. Chem. Soc.*, 2005, **127**, 17982–17983.
29 Z. Al-Ahmady and K. Kostarelos, Chemical components for the design of temperature-responsive vesicles as cancer therapeutics, *Chem. Rev.*, 2016, **116**, 3883–3918.
30 Z. Zhu and S. A. Sukhishvili, Temperature-Induced Swelling and Small Molecule Release with Hydrogen-Bonded Multilayers of Block Copolymer Micelles, *ACS Nano*, 2009, **3**, 3595–3605.
31 S. Qin, Y. Geng, D. E. Discher and S. Yang, Temperature-Controlled Assembly and Release from Vesicles of Poly(ethylene oxide)-*block*-Poly(*N*-isopropylacrylamide), *Adv. Mater.*, 2006, **18**, 2905–2909.
32 Y. Li, B. S. Lokitz and C. L. McCormick, Thermally Responsive Vesicles and Their Structural ''Locking'' through Polyelectrolyte Complex Formation, *Angew. Chem., Int. Ed.*, 2006, **118**, 5924–5927.
33 L. Xu, Z. Zhu and S. A. Sukhishvili, Polyelectrolyte Multilayers of Diblock Copolymer Micelles with Temperature-Responsive Cores, *Langmuir*, 2011, **27**, 409–415.
34 K. N. Plunkett, X. Zhu, J. S. Moore and D. E. Leckband, PNIPAM chain collapse depends on the molecular weight and grafting density, *Langmuir*, 2006, **22**, 4259–4266.
35 R. Cheng, F. Meng, S. Ma, H. Xu, H. Liu, X. Jing and Z. Zhong, Reduction and temperature dual-responsive crosslinked polymersomes for targeted intracellular protein delivery, *J. Mater. Chem.*, 2011, **21**, 19013–19020.
36 W. Agut, A. Brûlet, C. Schatz, D. Taton and S. Lecommandoux, pH and Temperature Responsive Polymeric Micelles and Polymersomes by Self-Assembly of Poly[2-(dimethylamino)ethylmethacrylate]-*b*-Poly(glutamic acid) Double Hydrophilic Block Copolymers, *Langmuir*, 2010, **26**, 10546–10554.
37 A. S. Hoffman, Stimuli-Responsive Polymers: Biomedical Applications and Challenges for Clinical Translation, *Adv. Drug Delivery Rev.*, 2013, **65**, 10–16.
38 A. K. Shakya, A. Kumar and K. S. Nandakumar, Adjuvant Properties of a Biocompatible Thermo-Responsive Polymer of NIsopropylacrylamide in Autoimmunity and Arthritis, *J. R. Soc., Interface*, 2011, **8**, 1748–1759.
39 H. Vihola, A. Laukkanen, L. Valtola, H. Tenhu and J. Hirvonen, Cytotoxicity of thermosensitive polymers poly(N-isopropylacrylamide), poly(*N*-vinylcaprolactam) and amphiphilically modified poly(*N*-vinylcaprolactam), *Biomaterials*, 2005, **26**, 3055–3064.
40 S. Panja, G. Dey, R. Bharti, K. Kumari, T. K. Maiti, M. Mandal and S. Chattopadhyay, Tailor-made temperature-sensitive micelle for targeted and on-demand release of anticancer drugs, *ACS Appl. Mater. Interfaces*, 2016, **8**, 12063–12074.
41 S. Sun and P. Wu, Infrared spectroscopic insight into hydration behavior of poly(*N*-vinylcaprolactam) in water, *J. Phys. Chem. B*, 2011, **115**, 11609–11618.
42 V. Kozlovskaya and E. Kharlampieva, Self-Assemblies of Thermoresponsive Poly(*N*-vinylcaprolactam) Polymers for Applications in Biomedical Field, *ACS Appl. Polym. Mater.*, 2020, **2**, 26–39.
43 X. Liang, V. Kozlovskaya, C. P. Cox, Y. Wang, M. Saeed and E. Kharlampieva, Synthesis and Self-Assembly of Thermosensitive Double-hydrophilic Poly(*N*-vinylcaprolactam)-*b*-poly(*N*-vinyl-2-pyrrolidone) Diblock Copolymers, *J. Polym. Sci., Part A: Polym. Chem.*, 2014, **52**, 2725–2737.
44 V. Kozlovskaya, F. Liu, B. Xue, F. Ahmad, A. Alford, M. Saeed and E. Kharlampieva, Polyphenolic polymersomes of temperature-sensitive poly(*N*-vinylcaprolactam)-*block*-(poly(*N*-vinylpyrrolidone)) for anticancer therapy, *Biomacromolecules*, 2017, **18**, 2552–2563.
45 S. Kozanoğlu, T. Özdemir and A. Usanmaz, Polymerization of *N*-vinylcaprolactam and characterization of poly(*N*-vinylcaprolactam), *J. Macromol. Sci., Part A: Pure Appl. Chem.*, 2011, **48**, 467–477.
46 X. Liang, F. Liu, V. Kozlovskaya, Z. Palchak and E. Kharlampieva, Thermoresponsive micelles from double LCST-Poly(3-methyl-*N*-vinylcaprolactam) block copolymers for cancer therapy, *ACS Macro Lett.*, 2015, **4**, 308–311.
47 V. Kozlovskaya, F. Liu, Y. Yang, K. Ingle, S. Qian, G. V. Halade, V. S. Urban and E. Kharlampieva, Temperature-responsive polymersomes of poly(3-methyl-*N*-vinylcaprolactam)-*block*-poly(*N*-vinylpyrrolidone) to decrease doxorubicin-induced cardiotoxicity, *Biomacromolecules*, 2019, **20**, 3989–4000.
48 M. Aslam, B. Fakher, M. A. Ashraf, Y. Cheng, B. Wang and Y. Qin, Plant Low-Temperature Stress: Signaling and Response, *Agronomy*, 2022, **12**, 702.
49 W. T. Heller, M. J. Cuneo, L. M. Debeer-Schmitt, C. Do, L. He, L. Heroux, K. C. Littrell, S. V. Pingali, S. Qian, C. B. Stanley, V. S. Urban, B. Wu and W. Bras, The Suite of Small-angle neutron Scattering Instruments at Oak Ridge National Laboratory, *J. Appl. Crystallogr.*, 2018, **51**, 242–248.
50 S. R. Kline, Reduction and Analysis of SANS and USANS Data using IGOR Pro, *J. Appl. Crystallogr.*, 2006, **39**, 895–900.
51 M. D. Kim, S. A. Dergunov, A. G. Richter, J. Durbin, S. N. Shmakov, Y. Jia, S. Kenbeilova, Y. Orazbekuly, A. Kengpeiil, E. Lindner, S. V. Pingali, V. S. Urban, S. Weigand and E. Pinkhassik, Facile Directed Assembly of Hollow Polymer Nanocapsules within Spontaneously Formed Catanionic Surfactant Vesicles, *Langmuir*, 2014, **30**, 7061–7069.
52 A. G. Richter, S. A. Dergunov, B. Ganus, Z. Thomas, S. V. Pingali, V. Urban, Y. Liu, L. Porcar and E. Pinkhassik, Scattering Studies of Hydrophobic Monomers in Liposomal Bilayers: An Expanding Shell Model of Monomer Distribution, *Langmuir*, 2011, **27**, 3792–3797.
53 B. Hammouda, A New Guinier-Porod Model, *J. Appl. Cryst.*, 2010, **43**, 716–719.

54 G. Pound, J. M. McKenzie, R. F. M. Lange and B. Klumperman, Polymer-protein conjugates from x-aldehyde endfunctional poly(*N*-vinylpyrrolidone) synthesised *via* xanthate-mediated living radical polymerisation, *Chem. Commun.*, 2008, 3193–3195.
55 Y. Wei and M. J. A. Hore, Characterizing polymer structure with small-angle neutron scattering: A Tutorial, *J. Appl. Phys.*, 2021, **129**, 171101.
56 P. Ruckdeschel, M. Dulle, T. Honold, S. Förster, M. Karg and M. Retsch, Monodisperse hollow silica spheres: An in-depth scattering analysis, *Nano Res.*, 2016, **9**, 1366–1376.
57 E. Urinov, M. Y. Kirgizbayeva, A. S. Kosimov and S. S. Rashidova, Some conformational parameters of poly(vinylpyrrolidone), poly(vinylcaprolactam) and their copolymers in dilute solutions, *Polym. Sci. U.S.S.R.*, 1989, **31**, 666–672.